JOURNAL OF VIROLOGY, Apr. 2004, p. 3572–3577 Vol. 78, No. 7
0022-538X/04/$08.00+0 DOI: 10.1128/JVI.78.7.3572–3577.2004

Prior Infection and Passive Transfer of Neutralizing Antibody Prevent Replication of Severe Acute Respiratory Syndrome Coronavirus in the Respiratory Tract of Mice

Kanta Subbarao,[1]* Josephine McAuliffe,[1] Leatrice Vogel,[1] Gary Fahle,[2] Steven Fischer,[2] Kathleen Tatti,[3] Michelle Packard,[3] Wun-Ju Shieh,[3] Sherif Zaki,[3] and Brian Murphy[1]

Laboratory of Infectious Diseases, National Institute of Allergy and Infectious Diseases,[1] and Microbiology Service, Clinical Center,[2] National Institutes of Health, Bethesda, Maryland 20892, and Infectious Disease Pathology Activity, National Center for Infectious Diseases, Centers for Disease Control and Prevention, Atlanta, Georgia 30333[3]

Received 21 October 2003/Accepted 10 November 2003

Following intranasal administration, the severe acute respiratory syndrome (SARS) coronavirus replicated to high titers in the respiratory tracts of BALB/c mice. Peak replication was seen in the absence of disease on day 1 or 2, depending on the dose administered, and the virus was cleared within a week. Viral antigen and nucleic acid were detected in bronchiolar epithelial cells during peak viral replication. Mice developed a neutralizing antibody response and were protected from reinfection 28 days following primary infection. Passive transfer of immune serum to naïve mice prevented virus replication in the lower respiratory tract following intranasal challenge. Thus, antibodies, acting alone, can prevent replication of the SARS coronavirus in the lung, a promising observation for the development of vaccines, immunotherapy, and immunoprophylaxis regimens.

Severe acute respiratory syndrome (SARS) is a severe respiratory illness caused by a newly identified virus, the SARS coronavirus (SARS-CoV) (2, 6, 8, 13). The disease emerged in southern China in late 2002 and spread to several countries within Asia and to Europe and North America in early 2003. The syndrome is characterized by fever, chills or rigors, headache, and nonspecific symptoms such as malaise and myalgias, followed by cough and dyspnea (2, 5, 15). According to the World Health Organization, 8,437 cases of SARS had been identified worldwide as of 11 July 2003 and 813 patients had died, resulting in an overall mortality rate of 9.6% (World Health Organization, http://www.who.int/csr/sars/country/2003_07_11). Respiratory tract disease progresses to acute respiratory distress syndrome, requiring intensive care and mechanical ventilation for more than 20% of patients (9, 15, 16). Prolonged hospitalizations associated with complications have been reported (9, 15). Public health measures, including early admission, contact tracing, quarantine, and travel restrictions, were instituted to control the spread of the disease (5), and the World Health Organization declared that the outbreak was over in July 2003.

The severe morbidity and mortality associated with SARS make it imperative that effective means to prevent and treat the disease be developed and evaluated, especially since it is not known whether the virus will reappear and exhibit a seasonal pattern of circulation like other respiratory virus pathogens or whether it will be independently reintroduced into the human population. Prevention and treatment strategies can be developed based on principles that apply to other pathogens, but evaluation of the efficacy of these strategies requires animal models.

* Corresponding author. Mailing address: Laboratory of Infectious Diseases, NIAID, Bldg. 50, Room 6132, 50 South Dr., MSC 8007, Bethesda, MD 20892. Phone: (301) 451-3839. Fax: (301) 496-8312. E-mail: Ksubbarao@niaid.nih.gov.

Coronaviruses are generally restricted in their host range, and viruses associated with disease in one species can be limited in their ability to replicate in other species (reviewed in reference 12). SARS-CoV differs from this general pattern because it is likely an animal virus that infects humans. Although closely related viruses have been isolated from animal species in southern China, it is not clear which animal species represents the reservoir from which the virus entered the human population (11). Cynomolgus macaques have been reported to develop pathological findings of pneumonia and have been proposed as an animal model for SARS (14). However, small-animal models, such as rodents, would be very useful for evaluating vaccines, immunotherapies, and antiviral drugs, and we have identified the mouse as a useful animal model for this purpose.

MATERIALS AND METHODS

Virus and cells. L. J. Anderson and T. G. Ksiazek from the Centers for Disease Control and Prevention (CDC), Atlanta, Ga., kindly provided the SARS-CoV (Urbani strain) used in this study (13). The virus was isolated and passaged twice in Vero E6 cells at the CDC and was passaged in Vero cells for two additional passages in our laboratory to generate a virus stock with a titer of $10^{6.5}$ 50% tissue culture infective doses ($TCID_{50}$)/ml. The Vero cells were maintained in OptiPro SFM (Invitrogen, Carlsbad, Calif.). All work with infectious virus was performed inside a biosafety cabinet, in a biosafety containment level 3 facility, and personnel wore powered air-purifying respirators (HEPA AirMate; 3M, Saint Paul, Minn.).

Animal studies. The mouse studies were approved by the National Institutes of Health Animal Care and Use Committee and were carried out in an approved animal biosafety level 3 facility. All personnel entering the facility wore powered air purifying respirators (HEPA AirMate). Female BALB/c mice 4 to 6 weeks old purchased from Taconic (Germantown, N.Y.) were housed four per cage. Mice that were lightly anesthetized with isoflurane were inoculated with 50 μl of diluted virus intranasally. On days 1, 2, 3, 5, 7, 9, and 11, mice were euthanized with carbon dioxide, and the lungs, nasal turbinates, and spleen were removed and stored at −70°C until the end of the study. In a separate experiment, mice were euthanized 2 days following virus administration, and the liver, kidneys, and part of the small intestine were removed and stored at −70°C. The frozen tissues were thawed and homogenized in a 10% (lungs, spleens, livers, kidneys, and

small intestines) or 5% (nasal turbinates) suspension in Leibovitz 15 medium (Invitrogen), and virus titers were determined in Vero cell monolayers in 24- and 96-well plates. Virus titers are expressed as $TCID_{50}$ per gram of tissue. A group of SARS-CoV-infected and mock-infected mice were weighed every other day until day 21. Mice that were administered 10^5 $TCID_{50}$ of SARS-CoV on day 0 were challenged with 10^3 or 10^5 $TCID_{50}$ of virus on day 28 to determine whether primary infection protected mice from subsequent challenge.

Postinfection hyperimmune serum was generated in four mice that received 10^5 $TCID_{50}$ of virus intranasally on day 0 and 10^7 $TCID_{50}$ of virus by the intraperitoneal and intranasal routes on day 28. Serum samples collected from these mice were pooled, and 200 μl was administered intraperitoneally to three naïve mice. A pool of nonimmune serum was collected from four uninfected mice and administered intraperitoneally to three naïve mice as a control. In the second passive transfer experiment, four mice received 500 μl of undiluted immune serum or nonimmune serum and three mice received a 1:10 dilution of immune serum. The mice were bled the next day to determine the level of neutralizing antibody achieved; three mice in each group were challenged with 10^4 $TCID_{50}$ of SARS-CoV intranasally, and all the mice were sacrificed 2 days later and their lungs and nasal turbinates were removed and homogenized in a 5% (wt/vol) suspension in Leibovitz 15 medium (Invitrogen). Virus titers were determined as described above.

The lungs from one mouse each that had received the undiluted immune serum or nonimmune serum but was not challenged with SARS-CoV were also homogenized in a 5% (wt/vol) suspension. SARS-CoV was added to the lung homogenates to achieve a titer of 10^5 $TCID_{50}$ per ml. Virus infectivity in the samples was assayed immediately and after incubation for 1 h on ice.

Neutralizing antibody assay. Twofold dilutions of heat-inactivated serum were tested in a microneutralization assay for the presence of antibodies that neutralized the infectivity of 100 $TCID_{50}$ of SARS-CoV in Vero cell monolayers, with four wells per dilution on a 96-well plate. The presence of viral cytopathic effect was read on days 3 and 4. The dilution of serum that completely prevented cytopathic effect in 50% of the wells was calculated by the Reed-Muench formula (26).

Histopathology. Mice were anesthetized with isoflurane and euthanized by cervical dislocation on day 2 or 9 following virus administration. The trachea was cannulated and ligated after the lungs were injected with 10% neutral buffered formalin. The tissues were then placed in 10% formalin, embedded in a paraffin block, and processed for routine histology.

Immunohistochemistry. A colorimetric immunoalkaline phosphatase immunohistochemistry method was developed with a mouse anti-SARS-CoV antibody (from P. Rollin, CDC). In brief, 3-μm sections from formalin-fixed, paraffin-embedded tissues were deparaffinized, rehydrated, and placed in an autostainer (Dako Corp., Carpinteria, Calif.). The sections were digested in 0.1 mg of proteinase K (Boehringer-Mannheim Corp., Indianapolis, Ind.) per ml and then incubated for 1 h with a hyperimmune mouse ascitic fluid reactive with SARS-CoV antigen at a 1:1,000 dilution. Optimal dilutions of the antibody and the requirement for predigestion were determined by a series of pilot studies performed on SARS-CoV-infected Vero cells. After incubation, the slides were washed and incubated with a biotinylated anti-mouse immunoglobulin antibody. Antigens were visualized by using a streptavidin-alkaline phosphatase complex, followed by naphthol-fast red substrate for colorimetric detection (Dako Corp.). Sections were counterstained with Mayer's hematoxylin (Fisher Scientific, Pittsburgh, Pa.).

In situ hybridization. Negative-sense riboprobes (approximately 625 and 325 bases in length) were generated from PCR products amplified from the nucleocapsid (N) and polymerase regions, respectively, of the SARS-CoV genome (P. A. Rota and B. Bankamp, CDC) and tailed with the T7 promoter. In vitro transcription to generate the probes was performed by incorporating digoxigenin-11-dUTP as described by Bankamp et al. (1), and in situ hybridization assays were performed essentially as described previously (3). Tissue sections were incubated with a pool of N and polymerase probes at a concentration of 2 ng/μl. The specificity of the SARS-CoV N and polymerase probes was determined by hybridizing the SARS-CoV probes to Vero E6 cells infected with SARS-CoV as well as to uninfected Vero E6 cells. In addition, the probes were hybridized to MRC-5 cells infected with human CoV (HCoV) OC43 and 229E and to uninfected tissues. Riboprobes of similar size, including positive-sense riboprobes directed against the same regions of N and polymerase portions of the SARS-CoV genome, the rotavirus Wa VP4 probe, and the metapneumovirus probe were incubated with SARS-CoV-infected cell controls and infected mouse tissue and served as negative controls.

Detection of viral nucleic acid. RNA was extracted from 100 μl of serial 10-fold dilutions of lung homogenates prepared in Leibovitz 15 medium with a NucliSens nucleic acid isolation kit (BioMerieux, Inc., Durham, N.C.). A 393-bp region of the SARS-CoV genome was amplified by reverse transcription (RT)-PCR with a LightCycler-RNA master hybridization probe kit (Roche Diagnostics) with primer pairs modified by the addition of two nucleotides from those described by Poutanen et al. (23) and 45 cycles. The results obtained with these primers were confirmed by amplification of a 348-bp fragment of the SARS-CoV genome with the primers described by Ksiazek et al. (13). RT-PCR products were detected with a pair of specific fluorophore-labeled hybridization probes on the LightCycler instrument (Roche Diagnostics).

Statistics. Log-transformed virus titers were compared in a two-tailed *t* test, and statistical significance was assigned to differences with P values of <0.05. Regression analysis was performed with Sigmaplot software between log-transformed neutralizing antibody titers in serum and virus titers in the respiratory tract.

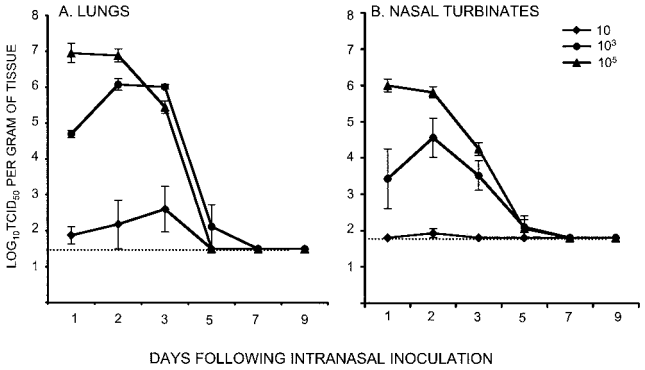

FIG. 1. Kinetics and dose-response of SARS-CoV replication in the respiratory tract of mice. The graphs show the mean titers of virus detected on the indicated days in the lower respiratory tract (A) and upper respiratory tract (B) of four BALB/c mice per group following intranasal administration of the indicated doses of SARS-CoV. Error bars associated with each data point indicate standard errors, and the dotted line indicates the lower limit of detection of virus in 10% (wt/vol) (lungs) and 5% (wt/vol) (nasal turbinates) suspensions.

RESULTS

Replication of SARS-CoV in mice. SARS-CoV was administered to lightly anesthetized 4- to 6-week-old female BALB/c mice by the intranasal route. This route of infection was selected because SARS is a respiratory illness in humans. Intranasal infection of mice resulted in virus recovery from the upper and lower respiratory tract but not the spleen, liver, kidneys, or small intestine. Although the mice continued to gain weight (data not shown) and showed no evidence of disease, the virus replicated efficiently in the respiratory tract when administered at doses of 10^3 and 10^5 $TCID_{50}$ (Fig. 1). The kinetics of viral replication in the lungs and nasal turbinates correlated with the dose of virus administered. At a dose of 10^5 $TCID_{50}$, the virus reached titers of 10^7 $TCID_{50}$ per g of lung tissue, with a peak on day 1. At a dose of 10^3, the peak virus titer was 10-fold lower and was delayed by a day. The virus replicated poorly when administered at a dose of 10 $TCID_{50}$. In nearly all experiments, the virus replicated to higher titers in the lungs than in the nasal turbinates at all doses tested and was cleared from the respiratory tract by day 7.

Microscopic examination of the trachea, bronchus, lung, thymus, and heart on day 2 revealed mild and focal peribronchiolar mononuclear inflammatory infiltrates (Fig. 2A) with no significant histopathologic change in other organs. Viral antigens and nucleic acids were focally distributed in bronchiolar epithelial cells (Fig. 2B and D). The HCoV-SARS N and

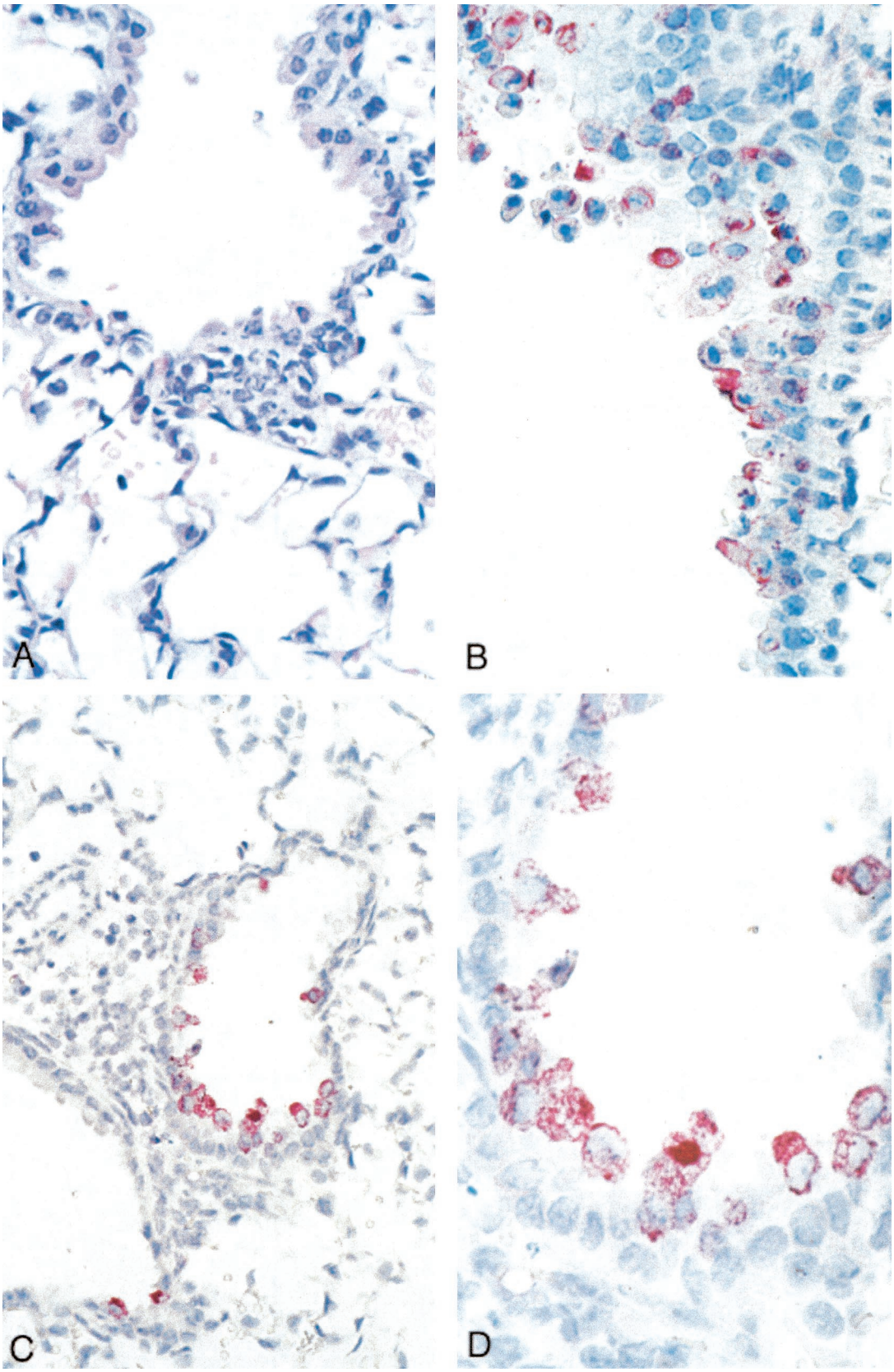

FIG. 2. Histopathology, immunohistochemistry, and in situ hybridization of mouse lung tissues harvested on day 2 following infection. (A) Focal and mild peribronchiolar mononuclear inflammatory infiltrate. Hematoxylin and eosin stain; magnification, ×158. (B) SARS-CoV antigens in multiple bronchiolar epithelial cells. Immunoalkaline phosphatase staining, naphthol-fast red substrate with light hematoxylin counterstain; original magnification, ×158. (C and D) SARS-CoV nucleic acids in multiple bronchiolar epithelial cells. Immunoalkaline phosphatase staining, naphthol-fast red substrate with light hematoxylin counterstain. Original magnification: C, ×100; D, ×250.

TABLE 1. Primary infection with SARS-CoV protects mice from subsequent challenge[a]

Primary infection inoculum ($TCID_{50}$)	Challenge dose ($TCID_{50}$)	Neutralizing antibody titer	Mean virus titer (log_{10} $TCID_{50}$/g) ± SE[b]	
			Lungs	Nasal turbinates
10^5	10^5	1:25*	1.6 ± 0.13*	≤1.8 ± 0*
	10^3	1:49*	≤1.5 ± 0[c]**	≤1.8 ± 0[d]*
0 (mock)	10^5	≤1:8	6.5 ± 0.18	5.4 ± 0.30
	10^3	≤1:4	4.5 ± 1.02	4.5 ± 0.18

[a] SARS-CoV challenge virus was administered intranasally 28 days following primary infection. Geometric mean neutralizing antibody titers in serum collected 28 days after primary infection were determined.
[b] *, $P < 0.05$ versus mock-infected control; **, $P = 0.058$ versus mock-infected control.
[c] Virus was not detected; this value represents the lower limit of detection of infectious virus in a 10% suspension.
[d] Virus was not detected; this value represents the lower limit of detection of infectious virus in a 5% suspension.

polymerase riboprobes hybridized only to lung tissue from infected mice (day 2) and to HCoV-SARS-infected Vero cells. Significant histopathology, viral antigen, and nucleic acids were not observed in the tissues of animals sacrificed on day 9.

Protection from subsequent challenge. Mice that had been infected with 10^5 $TCID_{50}$ of SARS-CoV were challenged 28 days later with 10^3 or 10^5 $TCID_{50}$ of SARS-CoV to determine if they developed resistance to reinfection. The level of replication of the challenge virus in the respiratory tract was determined on day 2, when virus replication should be close to the peak for each dose of virus. Primary infection provided a high level of resistance to replication of the challenge virus in both the upper and lower respiratory tract (Table 1). Each mouse developed neutralizing antibody in serum at 28 days following primary infection, with mean titers of 1:25 and 1:49 (Table 1). Thus, previous infection provided a high level of resistance in both the upper and lower respiratory tract.

Role of antibody in protection. We generated a small volume of hyperimmune serum (Table 2) by administering a second dose of SARS-CoV (10^7 $TCID_{50}$) via the intraperitoneal and intranasal routes to mice that had recovered from a primary infection. We transferred the serum to naïve mice in two separate experiments to determine whether antibody alone could prevent replication of SARS-CoV in the respiratory tract. Nonimmune serum from uninfected mice that lacked neutralizing antibody (Table 2) was administered to a control group. The mice received an intranasal challenge dose of 10^3 or 10^4 $TCID_{50}$ of SARS-CoV in experiments 1 and 2, respectively (Table 2). Mice that received immune serum were protected from replication of challenge virus, particularly in the lower respiratory tract (Table 2). Significant restriction of virus replication in the upper respiratory tract was noted in the mice in which passive transfer of undiluted hyperimmune serum resulted in a high titer (geometric mean titer, 1:231) of neutralizing antibodies (Table 2). There was an inverse correlation between the level of neutralizing antibody achieved in recipient mice and the virus titers in their lungs and nasal turbinates (r^2 values, 0.85 and 0.90, respectively, and $P < 0.005$ in both cases); complete protection of the lower respiratory tract was observed in mice with neutralizing antibody titers that exceeded 2^4 (1:16). The observation that viral replication was more effectively prevented in the lower respiratory tract than in the upper respiratory tract is consistent with findings in similar passive transfer experiments with influenza A viruses and respiratory syncytial virus (18, 24, 25).

Virus infectivity can be neutralized in vitro during tissue homogenization if a large amount of antibody is present (34). We found that antibody present in the lung homogenates of mice that received undiluted serum (experiment 2, Table 2) but were not challenged with SARS-CoV could partially neutralize exogenously added SARS-CoV from a titer of 10^5 $TCID_{50}$ per ml in the homogenate at time zero to $10^{2.5}$ $TCID_{50}$ per ml after an hour of incubation on ice, suggesting that it was possible that in vitro neutralization of virus during tissue homogenization could reduce the titer of infectious virus detected in the lung homogenates from mice that had received immune serum. The lower limits of detection of infectious virus in tissue homogenates indicated in Table 2 do not take into account the possibility of in vitro neutralization because the extent of in vitro neutralization varies depending on the amount of antibody present in the homogenate. Viral genetic material was detectable by RT-PCR in the lung homogenates with exogenously spiked SARS-CoV when the samples were diluted to 10^{-3} or 10^{-4}, corresponding to the detection of 1 to 10 infectious virus particles (Fig. 3). In contrast, lung homogenates from mice that received immune serum and were sub-

TABLE 2. Passive transfer of immune serum protects naïve mice from replication of challenge virus in the respiratory tract

Expt no. and dose of SARS-CoV ($TCID_{50}$)	Passively transferred serum[a]	Neutralizing antibody titer in serum[b]	Mean prechallenge neutralizing antibody titer in recipient mice	Virus replication in challenged mice			
				Lungs		Nasal turbinates	
				No. of mice infected/no. tested	Mean virus titer[c] ± SE	No. of mice infected/no. tested	Mean virus titer ± SE
1 (10^3)	Immune	1:284	1:28	0/3	≤1.5 ± 0[d]	2/3	3.2 ± 0.72
	Nonimmune	≤1:4	≤1:4	2/3	3.9 ± 1.21	2/3	2.4 ± 0.32
2 (10^4)	Immune, undiluted	1:1,024	1:231	0/3	≤1.8 ± 0[e]*	1/3	2.0 ± 0.17*
	Immune, 1:10 dilution	1:274	1:22	1/3	2.0 ± 0.17	2/3	3.3 ± 0.73
	Nonimmune	≤1:4	≤1:4	3/3	7.3 ± 0.14	3/3	5.6 ± 0.55

[a] Serum (200 μl) pooled from immunized or uninfected mice was administered to recipient mice by intraperitoneal injection in experiment 1, and 500 μl of the indicated serum preparation was administered to mice in experiment 2.
[b] Titer of antibody that neutralized infectivity of 100 $TCID_{50}$ of SARS-CoV.
[c] Virus titers are expressed as log_{10} $TCID_{50}$ per gram of tissue. *, $P < 0.05$ versus nonimmune control.
[d] Virus not detected; this value represents the lower limit of detection of infectious virus in a 10% suspension.
[e] Virus not detected; this value represents the lower limit of detection of infectious virus in a 5% suspension.

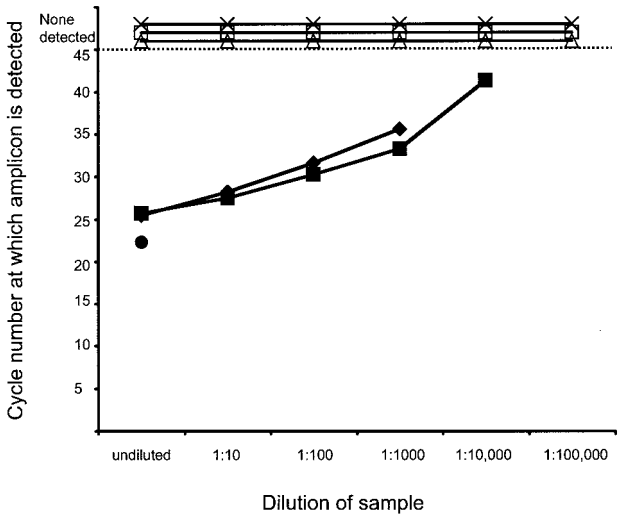

FIG. 3. Detection of viral nucleic acid in lung homogenates by RT-PCR. RNA extracted from serial 10-fold dilutions of lung homogenates obtained from mice that received passive transfers of immune or nonimmune serum was subjected to RT-PCR. For each dilution, the cycle number at which amplicons were detected is indicated. SARS-CoV nucleic acid was not detected at 45 cycles (dotted line) in lung homogenates from three mice (×, △, and □) that received passive transfers of immune serum but was detected in the virus stock (●) and also when virus was added exogenously to lung homogenates from mice that had received immune serum (◆) or nonimmune serum (■).

sequently challenged with SARS-CoV (experiment 2, Table 2) lacked both infectious virus and detectable viral nucleic acid (Fig. 3), indicating that the replication of SARS-CoV was restricted in these mice by the passively transferred neutralizing antibody.

DISCUSSION

The pattern of replication of SARS-CoV in the respiratory tract of mice resembles that of other human respiratory viruses, including respiratory syncytial virus and non-mouse-adapted human influenza A viruses administered to mice of a similar age in similar doses, in that it replicates in the respiratory tract of rodents in the absence of clinical illness (10, 27, 28). Although pathogenesis cannot be studied in the absence of clinical illness or disease, mouse models have been used to evaluate vaccine efficacy for viruses such as respiratory syncytial virus and influenza A virus that replicate to high titers in mice (4, 19). It might be possible to increase the virulence of SARS-CoV for mice by serial passage of the virus in this species, as has been done for influenza A viruses (35); alternatively, the administration of larger quantities of virus or the use of older mice might result in disease, as has been seen for respiratory syncytial virus (10, 28). Our data indicate that SARS-CoV replicates to a high enough titer that we will be able to evaluate vaccines and antiviral agents in this model. A large number of infected bronchiolar epithelial cells were identified in the lungs on day 2 by immunohistochemistry and in situ hybridization, when viral replication was at its peak. The mouse model will also facilitate the identification of host immune mechanisms that contribute to the resolution of SARS-CoV infection by testing the ability of the virus to replicate and cause disease in mice with specific targeted immune defects (7, 35).

Although SARS-specific antibody responses have been detected in convalescent-phase patient serum (13, 22), it is not known whether people who recovered from SARS would be protected from reinfection should a SARS epidemic recur, because primary infections with human and animal coronaviruses do not always protect the host from reinfection (reviewed in reference 12). It was reassuring that there was no evidence of enhanced SARS-CoV replication in mice upon reinfection or after the administration of immune serum. It was uncertain if these outcomes would occur because accelerated and fulminant disease has been observed in seropositive cats that were reexposed to a feline coronavirus, feline infectious peritonitis virus (reviewed in reference 20). Specifically, this accelerated and exacerbated disease occurred upon feline infectious peritonitis virus challenge in seropositive cats following prior infection (21, 32, 33), passive transfer of immune serum (21, 31), or vaccination (30). This phenomenon has been described as being similar to the antibody-mediated immune enhancement seen in dengue hemorrhagic fever (31). Vaughn et al. recently reported higher levels of virus replication in patients that developed dengue hemorrhagic fever (29) than in patients with uncomplicated dengue fever; such quantitative virology data have not been reported in immune-enhanced disease due to feline infectious peritonitis virus. If increased viral replication is also a feature of coronavirus-associated immune enhancement, the absence of viral replication in the respiratory tract of mice following SARS-CoV reinfection would argue against immune-enhanced disease as a threat in vaccinees or during SARS reinfection.

The rapid time course of SARS-CoV replication in mice is notable for two reasons. First, the pattern does not parallel that seen in humans; replication peaks early in mice and other animal models for SARS, including monkeys, ferrets, and cats (14, 17). In contrast, the viral load in the respiratory tract of humans peaks on day 10 (22). Second, the rapid replication kinetics and clearance of virus in mice may limit the use of this animal model for evaluation of vaccines that induce protection through cellular immune responses. However, the model will be useful for the evaluation of vaccines that mediate protection through antibodies.

In summary, SARS-CoV replicates in the respiratory tract of BALB/c mice to levels that will permit an evaluation of the efficacy of vaccines and immunotherapeutic and treatment strategies. Our observations in this mouse model, that primary infection provides protection from reinfection and that antibody alone can protect against viral replication, suggest that vaccines that induce neutralizing antibodies and strategies for immunoprophylaxis or, perhaps, immunotherapy are likely to be effective for SARS.

ACKNOWLEDGMENTS

We are grateful to the staff of the Building 50 Shared Animal Facility, NIAID, for assisting with the animal studies. We also thank Jeltley Montague for tissue processing and Jeannette Guarner and Christopher Paddock for help in evaluation of the histopathology, immunohistochemistry, and in situ hybridization studies.

REFERENCES

1. **Bankamp, B., S. Kearney, X. Liu, W. J. Bellini, and P. A. Rota.** 2002. Activity of polymerase proteins of vaccine and wild-type measles in a mini-genome replication assay. J. Virol. **76:**7073–7081.
2. **Booth, C. M., L. M. Matukas, G. A. Tomlinson, A. R. Rachlis, D. B. Rose, H. A. Dwosh, S. L. Walmsley, T. Mazzulli, M. Avendano, P. Derkach, I. E. Ephtimios, I. Kitai, B. D. Mederski, S. B. Shadowitz, W. L. Gold, L. A. Hawryluck, E. Rea, J. S. Chenkin, D. W. Cescon, S. M. Poutanen, and A. S. Detsky.** 2003. Clinical features and short-term outcomes of 144 patients with SARS in the greater Toronto area. JAMA **289:**2801–2809.
3. **Burt, F. J., R. Swanepoel, W. J. Shieh, J. F. Smith, P. A. Leman, P. W. Greer, L. M. Coffield, P. E. Rollin, T. G. Ksiazek, C. J. Peters, and S. R. Zaki.** 1997. Immunohistochemical and in situ localization of Crimean-Congo hemorrhagic fever (CCHF) virus in human tissues and implications for CCHF pathogenesis. Arch. Pathol. Lab. Med. **121:**839–846.
4. **Crowe, J. E., Jr., P. T. Bui, W. T. London, A. R. Davis, P. P. Hung, R. M. Chanock, and B. R. Murphy.** 1994. Satisfactorily attenuated and protective mutants derived from a partially attenuated cold-passaged respiratory syncytial virus mutant by introduction of additional attenuating mutations during chemical mutagenesis. Vaccine **12:**691–699.
5. **Donnelly, C. A., A. C. Ghani, G. M. Leung, A. J. Hedley, C. Fraser, S. Riley, L. J. Abu-Raddad, L. M. Ho, T. Q. Thach, P. Chau, K. P. Chan, T. H. Lam, L. Y. Tse, T. Tsang, S. H. Liu, J. H. Kong, E. M. Lau, N. M. Ferguson, and R. M. Anderson.** 2003. Epidemiological determinants of spread of causal agent of severe acute respiratory syndrome in Hong Kong. Lancet **361:**1761–1766.
6. **Drosten, C., S. Gunther, W. Preiser, S. van der Werf, H. R. Brodt, S. Becker, H. Rabenau, M. Panning, L. Kolesnikova, R. A. Fouchier, A. Berger, A. M. Burguiere, J. Cinatl, M. Eickmann, N. Escriou, K. Grywna, S. Kramme, J. C. Manuguerra, S. Muller, V. Rickerts, M. Sturmer, S. Vieth, H. D. Klenk, A. D. Osterhaus, H. Schmitz, and H. W. Doerr.** 2003. Identification of a novel coronavirus in patients with severe acute respiratory syndrome. N. Engl. J. Med. **348:**1967–1976.
7. **Epstein, S. L., C. Y. Lo, J. A. Misplon, C. M. Lawson, B. A. Hendrickson, E. E. Max, and K. Subbarao.** 1997. Mechanisms of heterosubtypic immunity to lethal influenza A virus infection in fully immunocompetent, T cell-depleted, beta2-microglobulin-deficient, and J chain-deficient mice. J. Immunol. **158:**1222–1230.
8. **Fouchier, R. A., T. Kuiken, M. Schutten, G. van Amerongen, G. J. van Doornum, B. G. van den Hoogen, M. Peiris, W. Lim, K. Stohr, and A. D. Osterhaus.** 2003. Aetiology: Koch's postulates fulfilled for SARS virus. Nature **423:**240.
9. **Fowler, R. A., S. E. Lapinsky, D. Hallett, A. S. Detsky, W. J. Sibbald, A. S. Slutsky, T. E. Stewart, and SARS Critical Care Group. Toronto.** 2003. Critically ill patients with severe acute respiratory syndrome. JAMA **290:** 367–373.
10. **Graham, B. S., M. D. Perkins, P. F. Wright, and D. T. Karzon.** 1988. Primary respiratory syncytial virus infection in mice. J. Med. Virol. **26:**153–162.
11. **Guan, Y., B. J. Zheng, Y. Q. He, X. L. Liu, Z. X. Zhuang, C. L. Cheung, S. W. Luo, P. H. Li, L. J. Zhang, Y. J. Guan, K. M. Butt, K. L. Wong, K. W. Chan, W. Lim, K. F. Shortridge, K. Y. Yuen, J. S. M. Peiris, and L. L. M. Poon.** 2003. Isolation and characterization of viruses related to the SARS coronavirus from animals in southern China. Science **302:**276–278.
12. **Holmes, K. V.** 2003. SARS coronavirus: a new challenge for prevention and therapy. J. Clin. Investig. **111:**1605–1609.
13. **Ksiazek, T. G., D. Erdman, C. S. Goldsmith, S. R. Zaki, T. Peret, S. Emery, S. Tong, C. Urbani, J. A. Comer, W. Lim, P. E. Rollin, S. F. Dowell, A. E. Ling, C. D. Humphrey, W. J. Shieh, J. Guarner, C. D. Paddock, P. Rota, B. Fields, J. DeRisi, J. Y. Yang, N. Cox, J. M. Hughes, J. W. LeDuc, W. J. Bellini, L. J. Anderson, and the SARS Working Group.** 2003. A novel coronavirus associated with severe acute respiratory syndrome. N. Engl. J. Med. **348:**1953–1966.
14. **Kuiken, T., R. A. M. Fouchier, M. Schutten, G. F. Rimmelzwaan, G. van Amerongen, D. van Riel, J. D. Laman, T. de Jong, G. van Doornum, W. Lim, A. E. Ling, P. K. S. Chan, J. S. Tam, M. C. Zambon, R. Gopal, C. Drosten, S. van der Werf, N. Escriou, J. C. Manuguerra, K. Stohr, J. S. M. Peiris, and A. D. M. E. Osterhaus.** 2003. Newly discovered coronavirus as the primary cause of severe acute respiratory syndrome. Lancet **362:**263–270.
15. **Lee, N., D. Hui, A. Wu, P. Chan, P. Cameron, G. M. Joynt, A. Ahuja, M. Y. Yung, C. B. Leung, K. F. To, S. F. Lui, C. C. Szeto, S. Chung, and J. J. Sung.** 2003. A major outbreak of severe acute respiratory syndrome in Hong Kong. N. Engl. J. Med. **348:**1986–1994.
16. **Lew, T. W., T. K. Kwek, D. Tai, A. Earnest, S. Loo, K. Singh, K. M. Kwan, Y. Chan, C. F. Yim, S. L. Bek, A. C. Kor, W. S. Yap, Y. R. Chelliah, Y. C. Lai, and S. K. Goh.** 2003. Acute respiratory distress syndrome in critically ill patients with severe acute respiratory syndrome. JAMA **290:**374–380.
17. **Martina, B. E. E., B. L. Haagmans, T. Kuiken, R. A. M. Fouchier, G. F. Rimmelzwaan, G. V. Amerongen, J. S. M. Peiris, W. Lim, and A. D. M. E. Osterhaus.** 2003. SARS virus infection of cats and ferrets. Nature **425:**915.
18. **Murphy, B. R.** 1999. Mucosal immunity to viruses, p. 695–707. *In* P. L. Ogra et al. (ed.), Mucosal immunology, 2nd ed. Academic Press, Inc., New York, N.Y.
19. **Novak, M., Z. Moldoveanu, D. P. Schafer, J. Mestecky, and R. W. Compans.** 1993. Murine model for evaluation of protective immunity to influenza virus. Vaccine **11:**55–60.
20. **Olsen, C. W.** 1993. A review of feline infectious peritonitis virus: molecular biology, immunopathogenesis, clinical aspects and vaccination. Vet. Microbiol. **36:**1–37.
21. **Pederson, N. C., and J. F. Boyle.** 1980. Immunologic phenomena in the effusive form of feline infectious peritonitis. Am. J. Vet. Res. **41:**868–876.
22. **Peiris, J. S., C. M. Chu, V. C. Cheng, K. S. Chan, I. F. Hung, L. L. Poon, K. I. Law, B. S. Tang, T. Y. Hon, C. S. Chan, K. H. Chan, J. S. Ng, B. J. Zheng, W. L. Ng, R. W. Lai, Y. Guan, K. Y. Yuen, and Hong Kong University/United Christian Hospital SARS Study Group.** 2003. Clinical progression and viral load in a community outbreak of coronavirus-associated SARS pneumonia: a prospective study. Lancet **361:**1767–1772.
23. **Poutanen, S. M., D. E. Low, B. Henry, S. Finkelstein, D. Rose, K. Green, R. Tellier, R. Draker, D. Adachi, M. Ayers, A. K. Chan, D. M. Skowronski, I. Salit, A. E. Simor, A. S. Slutsky, P. W. Doyle, M. Krajden, M. Petric, R. C. Brunham, A. J. McGeer, Canadian National Microbiology Laboratory, and the Canadian Severe Acute Respiratory Syndrome Study Team.** 2003. Identification of severe acute respiratory syndrome in Canada. N. Engl. J. Med. **348:**1995–2005.
24. **Prince, G. A., R. L. Horswood, and R. M. Chanock.** 1985. Quantitative aspects of passive immunity to respiratory syncytial virus infection in infant cotton rats. J. Virol. **55:**517–520.
25. **Ramphal, R., R. C. Cogliano, J. W. Shands, and P. A. Small.** 1979. Serum antibody prevents lethal murine influenza pneumonitis but not tracheitis. Infect. Immun. **25:**992–997.
26. **Reed, L. J., and H. Muench.** 1938. A simple method of estimating fifty per cent endpoints. Am. J. Hyg. **27:**493–497.
27. **Renegar, K. B.** 1992. Influenza virus infections and immunity: a review of human and animal models. Lab. Anim. Sci. **42:**222–232.
28. **Stack, A. M., R. Malley, R. A. Saladino, J. B. Montana, K. L. MacDonald, and D. C. Molrine.** 2000. Primary respiratory syncytial virus infection: pathology, immune response, and evaluation of vaccine challenge strains in a new mouse model. Vaccine **18:**1412–1418.
29. **Vaughn, D. W., S. Green, S. Kalayanarooj, B. L. Innis, S. Nimmannitya, S. Suntayakorn, T. P. Endy, B. Raengsakulrach, A. L. Rothman, F. A. Ennis, and A. Nisalak.** 2000. Dengue viremia titer, antibody response pattern, and virus serotype correlate with disease severity. J. Infect. Dis. **181:**2–9.
30. **Vennema, H., R. J. de Groot, D. A. Harbour, M. Dealderup, T. Gruffydd-Jones, M. C. Horzinek, and W. J. M. Spaan.** 1990. Early death after feline infectious peritonitis virus challenge due to recombinant vaccinia virus immunization. J. Virol. **64:**1407–1409.
31. **Weiss, R. C., and F. W. Scott.** 1981. Antibody-mediated enhancement of disease in feline infectious peritonitis: comparison with dengue hemorrhagic fever. Comp. Immunol. Microbiol. Infect. Dis. **4:**175–189.
32. **Weiss, R. C., and F. W. Scott.** 1981. Pathogenesis of feline infectious peritonitis: nature and development of viremia. Am. J. Vet. Res. **42:**382–390.
33. **Weiss, R. C., and F. W. Scott.** 1981. Pathogenesis of feline infectious peritonitis: pathologic changes and immunofluorescence. Am. J. Vet. Res. **42:** 2036–2048.
34. **Wells, M. A., F. A. Ennis, and P. Albrecht.** 1981. Recovery from a viral respiratory infection. II. Passive transfer of immune spleen cells to mice with influenza pneumonia. J. Immunol. **126:**1042–1046.
35. **Wyde, P. R., R. B. Couch, B. F. Mackler, T. R. Cate, and B. M. Levy.** 1977. Effects of low- and high-passage influenza virus infection in normal and nude mice. Infect. Immun. **15:**221–229.